

# Likelihood Non-Gaussianity in Large Scale Structure Analyses

ChangHoon Hahn, et al.

*Lawrence Berkeley National Laboratory, 1 Cyclotron Rd, Berkeley CA 94720, USA*

`changhoon.hahn@lbl.gov`

DRAFT --- 66905be --- 2017-12-05 --- NOT READY FOR DISTRIBUTION

## ABSTRACT

abstract here

*Subject headings:* methods: statistical — galaxies: statistics — methods: data analysis — cosmological parameters — cosmology: observations — large-scale structure of universe

## 1. Introduction

- Talk about the use of Bayesian parameter inference and getting the posterior in LSS cosmology
- Explain the two major assumptions that go into evaluating the likelihood
- Emphasize that we are not talking about non-Gaussian contributions to the likelihood
- Emphasize the scope of this paper is to address whether one of the assumptions matters for galaxy clustering analyses.

## 2. Gaussian Likelihood Assumption

- Depending on Hogg’s paper maybe a simple illustration of how the likelihood assumption

## 3. Mock Catalogs

Mock catalogs are play an indispensable role in standard cosmological analyses of LSS studies. They’re used for testing analysis pipelines ([Beutler et al. 2017](#); [Grieb et al. 2017](#); [Tinker & et al. in preparation](#)), testing the effect of systematics ([Guo et al. 2012](#); [Vargas-Magaña et al. 2014](#); [Hahn et al. 2017](#); [Pinol et al. 2017](#); [Ross et al. 2017](#)), and, most relevantly for this paper, estimating the covariance matrix ([Parkinson et al. 2012](#); [Kazin et al. 2014](#); [Grieb et al. 2017](#); [Alam et al. 2017](#); [Beutler et al. 2017](#); [Sinha et al. 2017](#)). In fact, nearly all current state-of-the-art LSS analyses use covariance matrices estimated from mocks to evaluate the likelihood for parameter inference.

While some argue for analytic estimates of the covariance matrix (e.g. [Mohammed et al. 2017](#)) or estimates directly from data by subsampling (e.g. [Norberg et al. 2009](#)), covariance matrices from mocks have a number of advantages. Mock catalogs allow us to incorporate detailed systematic errors present in the data and variance beyond the volume of the data. Even for analytic estimates, large ensembles of mocks are crucial for validation ([Slepian et al. 2017](#)). Moreover, as we show later in this paper, mock catalogs present an additional advantage: they allow us to quantify the non-Gaussianity of the likelihood and more accurately estimate the true likelihood.

In this paper, we focus on two LSS analyses: the powerspectrum multipole full shape analysis of [Beutler et al. \(2017\)](#) and group multiplicity function analysis of [Sinha et al. \(2017\)](#). Throughout the paper we will make extensive use of the mock catalogs used in these analyses. In this section, we give a brief description of these mocks and how the observables used in the analysis – *i.e.* the powerspectrum multipole ( $P_\ell$ ) and group multiplicity function ( $\zeta(N)$ ) – are calculated from them. Afterwards, we will describe how we compute the whitened data,  $\mathbf{X}^{\text{mock}}$ , and the covariance matrix,  $\mathbb{C}$ , from the mocks.

### 3.1. MultiDark-PATCHY Mock Catalog

In their powerspectrum multipole full shape analysis, [Beutler et al. \(2017\)](#) use the MultiDark-PATCHY mock catalogs from [Kitaura et al. \(2016\)](#). These mocks are generated using the PATCHY code ([Kitaura et al. 2014, 2015](#)). They rely on large-scale density fields generated using augmented Lagrangian Perturbation Theory (ALPT [Kitaura & Heß 2013](#)) on a mesh. This mesh is then populated with galaxies based on a combined non-linear deterministic and stochastic biases. The mocks from the PATCHYcode are then calibrated to reproduce the galaxy clustering in the high-fidelity BigMultiDark  $N$ -body simulation ([Rodríguez-Torres et al. 2016; Klypin et al. 2016](#)).

The galaxies are then assigned stellar masses using the HADRON code ([Zhao et al. 2015](#)). And the SUGAR code ([Rodríguez-Torres et al. 2016](#)) is applied to combine different boxes, incorporate selection effects and masking to produce mock light-cone galaxy catalogs. The statistics of the resulting mocks are then compared to observations and the process is iterated to reach desired accuracy. We refer readers to [Kitaura et al. \(2016\)](#) for further details.

In total, [Kitaura et al. \(2016\)](#) generated a 12,228 mock light-cone galaxy catalogs for BOSS Data Release 12: 2048 for each southern and northern galactic caps of LOWZ, CMASS, combined samples. In [Beutler et al. \(2017\)](#), they use 2045 and 2048 for the northern galactic cap (NGC) and southern galactic cap (SGC) of the LOWZ+CMASS combined sample. [Beutler et al. \(2017\)](#) excluded 3 mock realizations, due to notable issues, which have been since been addressed. Therefore, in our analysis we use all 2048 mocks for both the NGC and SGC of the LOWZ+CMASS combined sample.

### 3.2. Sinha et al. (2017) Mocks

The simulations used in the small-scale clustering analysis of Sinha et al. (2017) are from the Large Suite of Dark Matter Simulations project (LasDamas McBride et al. 2009). More specifically Sinha et al. (2017) uses the Consuelo and Carmen configurations, which were designed to model SDSS galaxies with  $M_r$  thresholds of  $-19$  and  $-21$ , respectively. The initial conditions for these simulations are derived from second order Lagrangian Perturbation Theory using the 2LTPIC code (Scoccimarro 1998; Crocce et al. 2006) and evolved using the  $N$ -body GADGET – 2 code (Springel 2005). Halos are then identified from the dark matter distribution outputs using the `ntropy – fofsv` code (Gardner et al. 2007), which uses a friend-of-friends algorithm (FoF Davis et al. 1985) with a linking length of 0.2 times the mean inter-particle separation. The FoF halo masses are then adjusted using the Warren et al. (2006) correction. The Consuelo simulation contains  $1400^3$  dark matter particles with mass of  $1.87 \times 10^9 h^{-1} M_\odot$  in a cubic volume of  $420 h^{-1} Mpc$  per side and is evolved from  $z_{\text{init}} = 99$ . The Carmen simulation contains  $1120^3$  dark matter particles with mass of  $4.938 \times 10^{10} h^{-1} M_\odot$  in a cubic volume of  $1000 h^{-1} Mpc$  per side and is evolved from  $z_{\text{init}} = 49$ . They use the following cosmological parameters, which are motivated by the WMAP3 constraints (Spergel et al. 2007):  $\Omega_m = 0.25$ ,  $\Omega_\Lambda = 0.75$ ,  $\Omega_b = 0.04$ ,  $h = 0.7$ ,  $\sigma_8 = 0.8$ , and  $n_s = 1.0$ .

The FoF halo catalogs are then populated with galaxies using the ‘Halo Occupation Distribution’ (HOD) framework. In this framework, the number, positions, and velocities of galaxies are described statistically by an HOD model. Sinha et al. (2017) adopts the ‘vanilla’ HOD model of Zheng et al. (2007), where the mean number of central and satellite galaxies are described by the halo mass and five HOD parameters:  $M_{\text{min}}$ ,  $\sigma_{\log M}$ ,  $M_0$ ,  $M_1$ , and  $\alpha$ . Finally, once the simulation boxes are populated with galaxies, observational systematic effects are imposed. The peculiar velocities of galaxies are used to impose redshift-space distortions. And galaxies that lie outside the redshift limits or sky footprint of the SDSS sample are removed. For further details regarding the LasDamas simulations or mock catalogs, we refer readers to Sinha et al. (2017).

To calculate their covariance matrix, Sinha et al. (2017) produced 200 independent mock catalogs from 50 simulations using a single set of HOD model parameters. To take advantage of the methods we present in this work (Sections ref), we require a large number of mock catalogs. Our methods rely on sampling multidimensional distributions, so incorporating more mocks into the analysis drastically improves their accuracy. Therefore, we utilize an additional 19,800 mock catalogs made from the procedure. These mocks are not generated using the same set of HOD model parameters, but 200 mocks each from 99 sets of HOD parameters sampled from the MCMC chain used to produce the posterior probability distribution presented in Sinha et al. (2017).

### 3.3. Mock Observable $\mathbf{X}^{\text{mock}}$ and Covariance Matrix $\mathbb{C}$

In [Beutler et al. \(2017\)](#) and [Sinha et al. \(2017\)](#) they analyze the powerspectrum multipoles measured from the BOSS DR12 galaxies and the group multiplicity function measured from the SDSS DR7 galaxies, respectively. To get from the mock catalogs described above to the covariance matrices used in these analyses, the observables must be consistently measured for each mock catalog. Below we briefly describe how  $P_\ell(k)$  and  $\zeta(N)$  are measured in [Beutler et al. \(2017\)](#) and [Sinha et al. \(2017\)](#) and how the covariance matrix is computed.

To measure the powerspectrum multipoles of the BOSS DR12 galaxies and the MutliDark-PATCHY mocks (Section 3.1), [Beutler et al. \(2017\)](#) uses a fast fourier transform (FFT) based anisotropic powerspectrum estimator based on [Bianchi et al. \(2015\)](#) and [Scoccimarro \(2015\)](#). This estimator estimates the monopole, quadrupole, and hexadecapole ( $\ell = 0, 2$ , and 4) of the powerspectrum using FFTs of the overdensity field multipoles for a given survey geometry. By using FFTs rather than counting all galaxy pairs, the estimator significantly reduces the computational costs to  $\mathcal{O}(N \log N)$ , where  $N$  is the number of grid cells used to bin the galaxy data. The powerspectrum multipoles are calculated in bins of  $\Delta k = 0.01 h\text{Mpc}^{-1}$ . The powerspectrum monopole and quadrupole are computed over the range  $k = 0.01 - 0.15 h\text{Mpc}^{-1}$  while the hexadecapole is computed over the range  $k = 0.01 - 0.10 h\text{Mpc}^{-1}$ . For further details on the estimator we refer readers to Section 3 of [?](#) .

Using the  $P_\ell(k)$  of the MultiDark-PATCHY mocks, [Beutler et al. \(2017\)](#) then computes the covariance matrix of all multipoles as

$$\mathbb{C}_{xy} = \frac{1}{N_{\text{mock}} - 1} \sum_{n=1}^{N_{\text{mock}}} [P_{\ell,n}(k_i) - \bar{P}_\ell(k_i)] \times [P_{\ell',n}(k_j) - \bar{P}_{\ell'}(k_j)]. \quad (1)$$

$N_{\text{mock}}$  is the number of mock catalogs and  $\bar{P}_\ell$  is the mean of the mock powerspectra:

$$\bar{P}_\ell(k_i) = \frac{1}{N_{\text{mock}}} \sum_{n=1}^{N_{\text{mock}}} P_{\ell,n}(k_i). \quad (2)$$

The  $(x, y)$  element of  $\mathbb{C}$  is given by  $(x, y) = (n_b \frac{\ell}{2} + i, n_b \frac{\ell'}{2} + j)$ , where  $n_b$  is the number of bins in each multipole power spectrum ( $n_b = 14$  for the monopole and quadrupole;  $n_b = 9$  for the hexadecapole).  $\mathbb{C}$  is a  $37 \times 37$  matrix.

In this work, we compute the  $P_\ell(k)$  of the MultiDark-PATCHY mocks, using a similar FFT-based estimator of [?](#)  instead of the estimator in [Beutler et al. \(2017\)](#). Our choice was based on computational convenience. A python implementation of the estimator is publicly available in the NBODYKIT package<sup>3</sup>. We emphasize that the resulting  $P_\ell(k)$ s and covariance matrix from the two estimators are consistent with one another.

---

<sup>3</sup><http://nbodykit.readthedocs.io/en/latest/index.html>

Next, for the [Sinha et al. \(2017\)](#) analysis, to compute the group multiplicity function, they use the ? friend-of-friend algorithm to identify groups in the SDSS and mock data. Based on this algorithm, a galaxy pair is assigned to the same group if their projected and line-of-sight separations are both less than the corresponding linking length. [Sinha et al. \(2017\)](#) adopts the ? linking lengths:  $b_{\perp} = 0.14$  and  $b_{\parallel} = 0.75$  times the mean inter-galaxy separation  $n_g^{-1/3}$ , where  $n_g$  is the number density of the sample. For reference, the linking lengths for the SDSS DR7  $M_r < -19$  sample correspond to comoving lengths of  $(r_{\perp}, r_{\parallel}) = (0.57, 3.05)h^{-1}\text{Mpc}$ . Once the groups are identified in the SDSS and mock data,  $\zeta(N)$  is derived by calculating the comoving number density of groups in bins of richness  $N$  *i.e.* the number of galaxies in the group. For the  $M_r < 19$  SDSS sample, [Sinha et al. \(2017\)](#) uses eight bins of  $N$ :  $(5 - 6), (7 - 9), (10 - 13), (14 - 19), (20 - 32), (33 - 52), (53 - 84), (85 - 220)$ . For further details we refer readers to Section 4.2 of [Sinha et al. \(2017\)](#).

In the rest of this paper we investigate the non-Gaussianity of the likelihood and its impact on parameter inference for the analysis in [Beutler et al. \(2017\)](#) and [Sinha et al. \(2017\)](#). In order to consistently discuss the two separate analyses, we define the  $\mathbf{X}^{\text{mock}}$  matrix and covariance matrix  $\mathbb{C}$  and describe how they are calculated from the mock catalogs described above.

$$\mathbf{X}_i = [P_0(k)_i, P_2(k)_i, P_4(k)_i] \quad (3)$$

Furthermore, **talk about the data whitening and what we mean by covariance matrix for GMF**  $\mathbf{X}_i = [P_0(k)_i, P_2(k)_i, P_4(k)_i]$   
 $\mathbf{X}_i = \zeta(N)_i$   
 $\mathbf{X} = \{\mathbf{X}_i\}$

#### 4. Quantifying the Likelihood non-Gaussianity

In [Sellentin et al. \(2017\)](#) **discuss how sellentin and hartlap's stuff is an attempt to quantify the divergence**

A more direct approach can be taken to quantify the non-Gaussianity of the likelihood. We can calculate the divergence between the distribution of our observable,  $p(x)$ , and  $q(x)$  a multivariate Gaussian described by the average of the mocks and the covariance matrix  $\mathbb{C}$ . The following are two of the most commonly used divergences: the Kullback-Leibler (hereafter KL) divergence

$$D_{KL}(p \parallel q) = \int p(x) \log \frac{p(x)}{q(x)} dx \quad (4)$$

and the Rényi- $\alpha$  divergence

$$D_{R-\alpha}(p \parallel q) = \frac{1}{\alpha - 1} \log \int p^{\alpha}(x) q^{1-\alpha}(x) dx. \quad (5)$$

In the limit as  $\alpha$  approaches 1, the Rényi- $\alpha$  divergence is equivalent to the KL divergence.

Of course, in our case, we don't know  $p(x)$  — *i.e.* the distribution of our observable. If we did, we would simply use that instead of bothering with the covariance matrix or this paper. We can, however, still estimate the divergence using nonparametric estimators (Wang et al. 2009; Póczos et al. 2012; Krishnamurthy et al. 2014). These estimators, allows us to estimate the divergence directly from samples  $X_{1:n} = \{X_1, \dots, X_n\}$  and  $Y_{1:m} = \{Y_1, \dots, Y_m\}$  drawn from  $p$  and  $q$  respectively:  $\hat{D}_\alpha(X_{1:n} \parallel Y_{1:m})$ .

For instance, the estimator presented in Póczos et al. (2012) allows us to estimate the kernel function of the Rényi- $\alpha$  divergence,

$$D_\alpha(p \parallel q) = \int p^\alpha(x) q^{1-\alpha}(x) dx. \quad (6)$$

using  $k$ th nearest neighbor density estimators. Let  $\rho_k(x)$  denote the Euclidean distance of the  $k$ th nearest neighbor of  $x$  in the sample  $X_{1:n}$  and  $\nu_k(x)$  denote the Euclidean distance of the  $k$ th nearest neighbor of  $x$  in the sample  $Y_{1:m}$ . Then  $D_\alpha(p \parallel q)$  can be estimated as

$$\hat{D}_\alpha(X_{1:n} \parallel Y_{1:m}) = \frac{B_{k,\alpha}}{n} \left( \frac{n-1}{m} \right)^{1-\alpha} \sum_{i=1}^n \left( \frac{\rho_k^d(X_i)}{\nu_k^d(X_i)} \right)^{1-\alpha}, \quad (7)$$

where  $B_{k,\alpha} = \frac{\Gamma(k)^2}{\Gamma(k-\alpha+1)\Gamma(k+\alpha-1)}$ . Póczos et al. (2012) goes to further prove that this estimated kernel function is asymptotically unbiased,

$$\lim_{n,m \rightarrow \infty} \mathbb{E}[\hat{D}_\alpha(X_{1:n} \parallel Y_{1:m})] = D_\alpha(p \parallel q). \quad (8)$$

Plugging  $\hat{D}_\alpha(X_{1:n} \parallel Y_{1:m})$  into Eq. 5, we get an estimator for the Rényi- $\alpha$  divergence. A similar estimator (Wang et al. 2009) can also be derived for the KL divergence (Eq. 4). We note that while the divergence estimators converge to the true divergence with a large enough samples, with a limited number of samples from the distribution, the estimators are noisy.

These divergence estimates have been applied to Support Vector Machines and used extensively in the machine learning and astronomical literature with great success **elaborate a lot more**

- Compile papers that use this divergence, Ntampaka et al. (2015, 2016)

For more details on the non-parametric divergence estimators, we refer readers to Póczos et al. (2012) and Krishnamurthy et al. (2014).

Now we can use the divergence estimators above to quantify the non-Gaussianity of the likelihood. More specifically, we're intersted in the divergence between the distribution  $p(x)$  sampled by the mock observables ( $\mathbf{X}^{\text{mock}}$ ) and the multivariate Gaussian distribution assumed in standard analyses, which is solely described by the mean and covariance calculated

from the mocks ( $\mathcal{N}(\overline{\mathbf{X}^{\text{mock}}}, \mathbf{C})$ ). Since  $\mathbf{X}^{\text{mock}}$  is a sample from  $p(x)$ , we draw a reference sample  $\mathbf{Y}^{\text{ref}}$  from  $\mathcal{N}(\overline{\mathbf{X}^{\text{mock}}}, \mathbf{C})$  to use in the estimators. Similar to the experiments detailed in [Póczos et al. \(2012\)](#), we construct  $\mathbf{Y}^{\text{ref}}$  with a comparable sample size as  $\mathbf{X}^{\text{mock}}$ : 2000 and 10,000 for the  $P_\ell$  and  $\zeta$  analyses respectively.

In Figure 2 we compare the distribution of Rényi- $\alpha$  (left) and  $KL$  (right) divergence estimates (orange)  $\hat{D}_{R\alpha}$  and  $\hat{D}_{KL}$  between the mock data  $\mathbf{X}^{\text{mock}}$  and a reference sample  $\mathbf{Y}^{\text{ref}}$  for the  $P_\ell(k)$  (top) and  $\zeta(N)$  (bottom) analyses. As a reference point for the comparison, we include in Figure 2 (blue) the distribution of Rényi- $\alpha$  and  $KL$  divergence estimates if  $\mathbf{X}^{\text{mock}}$  were actually sampled from  $\mathcal{N}(\overline{\mathbf{X}^{\text{mock}}}, \mathbf{C})$  and  $\mathbf{Y}^{\text{ref}}$ . All distributions were constructed using 100 divergence estimates.

The discrepancy between the blue and orange distributions illustrates the non-Gaussianity of  $p(x)$  sampled by  $\mathbf{X}^{\text{mock}}$ .

- Describe the discrepancy.

## 5. A More Accurate Likelihood

- Gaussian Mixture Model
- expectation maximization algorithm [Dempster et al. \(1977\)](#)
- Bayesian Information Criteria
- Figure illustrating both methods on highest N GMF bin

### 5.1. Independent Component Analysis

Curse of dimensionality! 2048 mocks in Beutler not enough to directly estimate the 37-dimensional space, so we use independent component analysis [Hartlap et al. \(2009\)](#)

- equation
- Similar figure to [Hartlap et al. \(2009\)](#) that tests the independence?
- Kernel Density Estimation
- 

Figure 2

## 6. Impact on Parameter Inference

### 6.1. MCMC

- details of each of the MCMC runs

### 6.2. Importance Sampling

- equations explaining importance sampling framework

Figure 3

Figure 4

## 7. Discussion

- Will it matter for future surveys?
- Likelihood free inference (cite justin’s paper)

## 8. Summary

### Acknowledgements

It’s a pleasure to thank Simone Ferraro, David W. Hogg, Emmaneul Schaan, Roman Scoc-  
cimarro Zachary Slepian

### REFERENCES

- Alam, S., Ata, M., Bailey, S., et al. 2017, [Monthly Notices of the Royal Astronomical Society](#), 470, 2617
- Beutler, F., Seo, H.-J., Saito, S., et al. 2017, [Monthly Notices of the Royal Astronomical Society](#), 466, 2242
- Bianchi, D., Gil-Marín, H., Ruggeri, R., & Percival, W. J. 2015, [Monthly Notices of the Royal Astronomical Society](#), 453, L11
- Crocce, M., Pueblas, S., & Scoccimarro, R. 2006, [Monthly Notices of the Royal Astronomical Society](#), 373, 369
- Davis, M., Efstathiou, G., Frenk, C. S., & White, S. D. M. 1985, [The Astrophysical Journal](#), 292, 371
- Dempster, A. P., Laird, N. M., & Rubin, D. B. 1977, *Journal of the Royal Statistical Society. Series B (Methodological)*, 39, 1
- Gardner, J. P., Connolly, A., & McBride, C. 2007, in *Astronomical Data Analysis Software and Systems XVI*, Vol. 376, 69



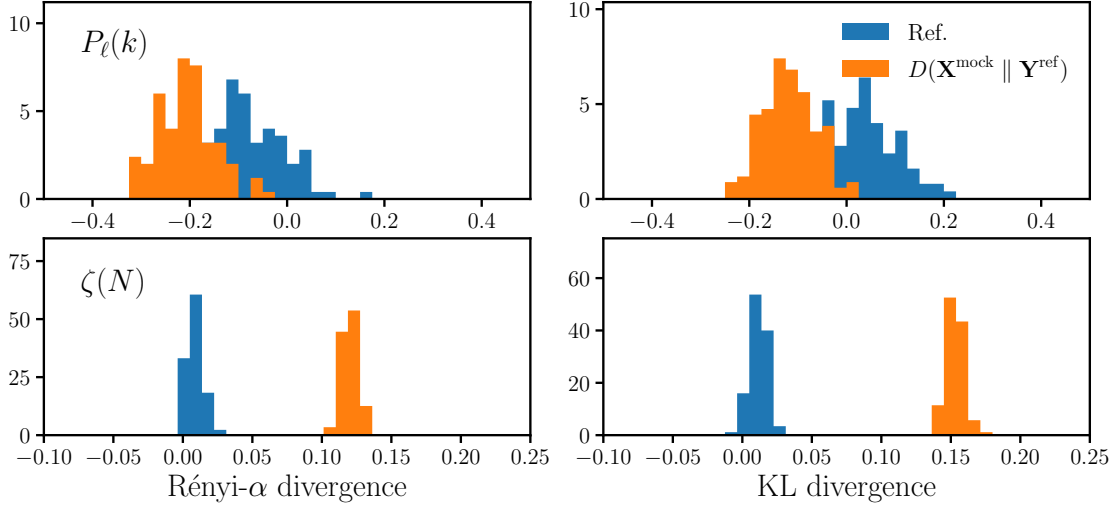


Fig. 1.— Rényi- $\alpha$  and KL divergence estimates, ( $D_{R\alpha}$  and  $D_{KL}$ ), between the mock data  $\mathbf{X}^{\text{mock}}$  and a reference sample  $\mathbf{Y}^{\text{ref}}$  for the  $P_\ell(k)$  (left) and  $\zeta(N)$  (right) analyses.

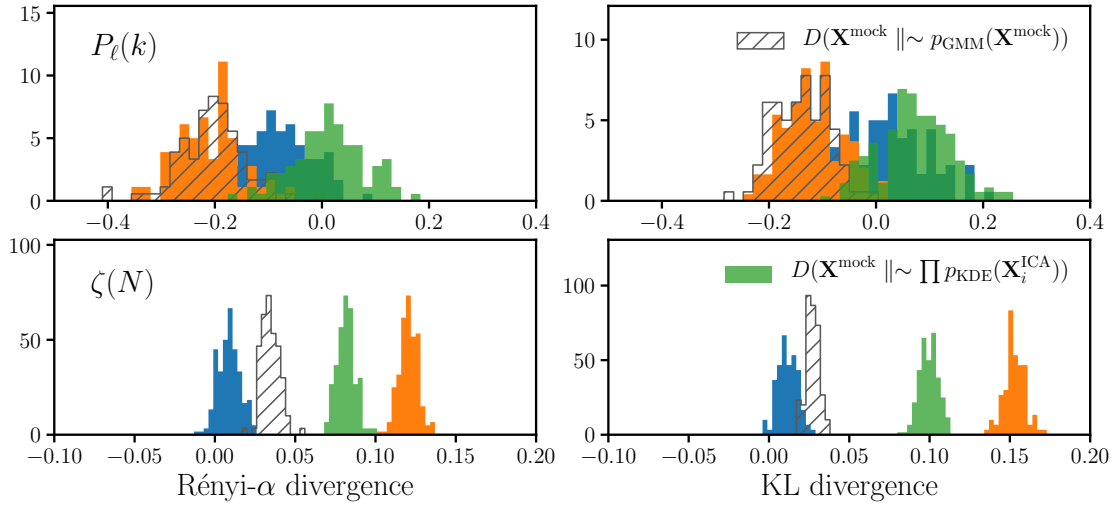


Fig. 2.—

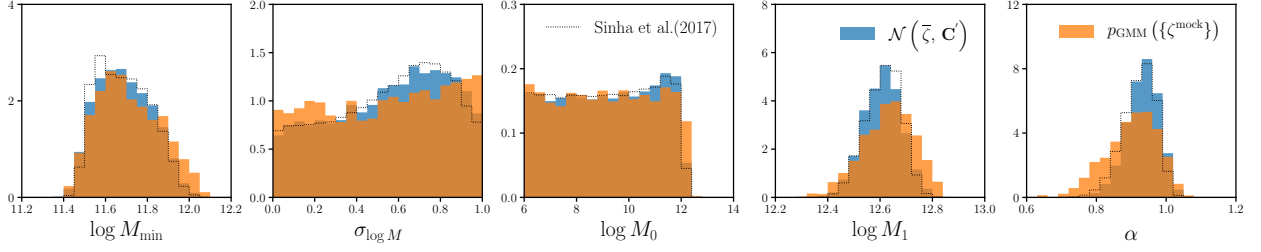


Fig. 3.—

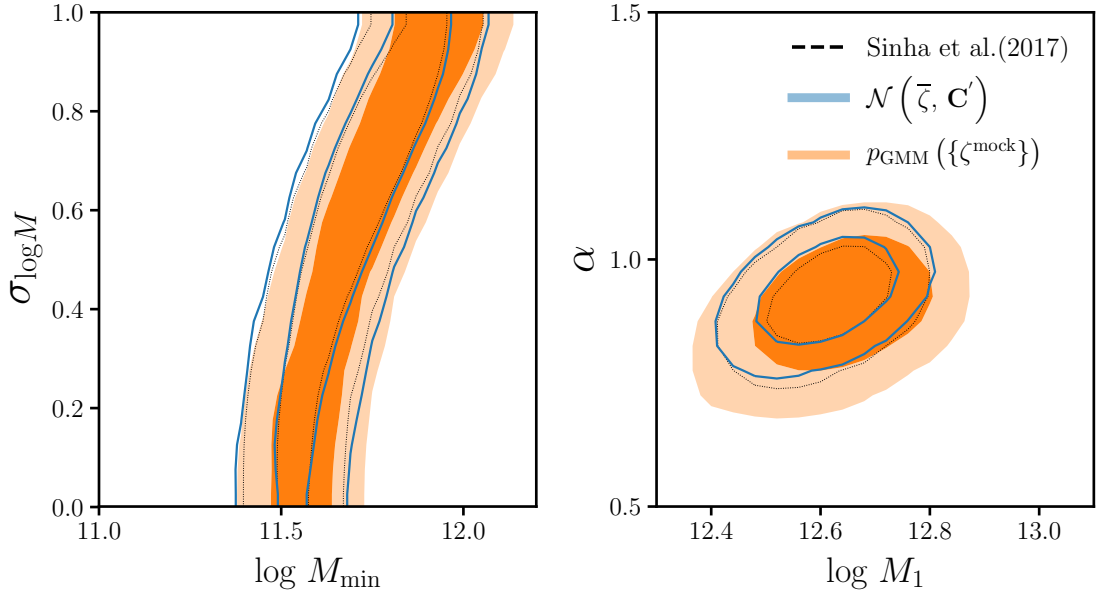


Fig. 4.—

- Grieb, J. N., Sánchez, A. G., Salazar-Albornoz, S., et al. 2017, [Monthly Notices of the Royal Astronomical Society](#), 467, 2085
- Guo, H., Zehavi, I., & Zheng, Z. 2012, [The Astrophysical Journal](#), 756, 127
- Hahn, C., Scoccimarro, R., Blanton, M. R., Tinker, J. L., & Rodríguez-Torres, S. A. 2017, [Monthly Notices of the Royal Astronomical Society](#), 467, 1940
- Hartlap, J., Schrabback, T., Simon, P., & Schneider, P. 2009, [Astronomy and Astrophysics](#), 504, 689
- Kazin, E. A., Koda, J., Blake, C., et al. 2014, [Monthly Notices of the Royal Astronomical Society](#), 441, 3524
- Kitaura, F.-S., Gil-Marín, H., Scóccola, C. G., et al. 2015, [Monthly Notices of the Royal Astronomical Society](#), 450, 1836
- Kitaura, F.-S., & Heß, S. 2013, [Monthly Notices of the Royal Astronomical Society](#), 435, L78
- Kitaura, F.-S., Yepes, G., & Prada, F. 2014, [Monthly Notices of the Royal Astronomical Society](#), 439, L21
- Kitaura, F.-S., Rodríguez-Torres, S., Chuang, C.-H., et al. 2016, [Monthly Notices of the Royal Astronomical Society](#), 456, 4156
- Klypin, A., Yepes, G., Gottlöber, S., Prada, F., & Heß, S. 2016, [Monthly Notices of the Royal Astronomical Society](#), 457, 4340
- Krishnamurthy, A., Kandasamy, K., Poczos, B., & Wasserman, L. 2014, arXiv:1402.2966 [math, stat], [arXiv:1402.2966 \[math, stat\]](#)
- McBride, C., Berlind, A., Scoccimarro, R., et al. 2009, in *Bulletin of the American Astronomical Society*, Vol. 213, 425.06
- Mohammed, I., Seljak, U., & Vlah, Z. 2017, [Monthly Notices of the Royal Astronomical Society](#), 466, 780
- Norberg, P., Baugh, C. M., Gaztañaga, E., & Croton, D. J. 2009, [Monthly Notices of the Royal Astronomical Society](#), 396, 19
- Ntampaka, M., Trac, H., Sutherland, D. J., et al. 2015, [The Astrophysical Journal](#), 803, 50
- . 2016, [The Astrophysical Journal](#), 831, 135
- Parkinson, D., Riemer-Sørensen, S., Blake, C., et al. 2012, [Physical Review D](#), 86, 103518
- Pinol, L., Cahn, R. N., Hand, N., Seljak, U., & White, M. 2017, [Journal of Cosmology and Astroparticle Physics](#), 2017, 008
- Póczos, B., Xiong, L., Sutherland, D. J., & Schneider, J. 2012, in [2012 IEEE Conference on Computer Vision and Pattern Recognition](#), 2989
- Rodríguez-Torres, S. A., Chuang, C.-H., Prada, F., et al. 2016, [Monthly Notices of the Royal Astronomical Society](#), 460, 1173
- Ross, A. J., Beutler, F., Chuang, C.-H., et al. 2017, [Monthly Notices of the Royal Astronomical Society](#), 464, 1168

- Scoccimarro, R. 1998, [Monthly Notices of the Royal Astronomical Society](#), 299, 1097
- . 2015, [Physical Review D](#), 92, 083532
- Sellentin, E., Jaffe, A. H., & Heavens, A. F. 2017, arXiv:1709.03452 [astro-ph, stat],  
[arXiv:1709.03452 \[astro-ph, stat\]](#)
- Sinha, M., Berlind, A. A., McBride, C. K., et al. 2017, arXiv:1708.04892 [astro-ph],  
[arXiv:1708.04892 \[astro-ph\]](#)
- Slepian, Z., Eisenstein, D. J., Brownstein, J. R., et al. 2017, [Monthly Notices of the Royal Astronomical Society](#), 469, 1738
- Spergel, D. N., Bean, R., Doré, O., et al. 2007, [The Astrophysical Journal Supplement Series](#), 170, 377
- Springel, V. 2005, [Monthly Notices of the Royal Astronomical Society](#), 364, 1105
- Tinker, J. L., & et al. in preparation
- Vargas-Magaña, M., Ho, S., Xu, X., et al. 2014, [Monthly Notices of the Royal Astronomical Society](#), 445, 2
- Wang, Q., Sanjeev, K., & Sergio, V. 2009, IEEE TRANSACTIONS ON INFORMATION THEORY, 55, 2392
- Warren, M. S., Abazajian, K., Holz, D. E., & Teodoro, L. 2006, [The Astrophysical Journal](#), 646, 881
- Zhao, C., Kitaura, F.-S., Chuang, C.-H., et al. 2015, [Monthly Notices of the Royal Astronomical Society](#), 451, 4266
- Zheng, Z., Coil, A. L., & Zehavi, I. 2007, [The Astrophysical Journal](#), 667, 760